

MIT Open Access Articles

Exploring the Behavior of Bovine Serum Albumin in Response to Changes in the Chemical Composition of Responsive Polymers: Experimental and Simulation Studies

The MIT Faculty has made this article openly available. **Please share** how this access benefits you. Your story matters.

Citation: Hsieh, Shih-Rong et al. "Exploring the Behavior of Bovine Serum Albumin in Response to Changes in the Chemical Composition of Responsive Polymers: Experimental and Simulation Studies." *Polymers* 8.6 (2016): 238.

As Published: <http://dx.doi.org/10.3390/polym8060238>

Publisher: MDPI AG

Persistent URL: <http://hdl.handle.net/1721.1/105923>

Version: Final published version: final published article, as it appeared in a journal, conference proceedings, or other formally published context

Terms of use: Creative Commons Attribution 4.0 International License



Article

Exploring the Behavior of Bovine Serum Albumin in Response to Changes in the Chemical Composition of Responsive Polymers: Experimental and Simulation Studies

Shih-Rong Hsieh ^{1,†}, P. Madhusudhana Reddy ^{2,†}, Chi-Jung Chang ^{2,*}, Awanish Kumar ³, Wan-Chi Wu ² and Hui-Yi Lin ⁴

¹ Department of Surgery, Taichung Veterans General Hospital, 1650 Taiwan Boulevard Section 4, Taichung 40705, Taiwan; Season@vghtc.gov.tw

² Department of Chemical Engineering, Feng Chia University, 100, Wenhwa Road, Seatwen, Taichung 40724, Taiwan; pmsreddy86@gmail.com (P.M.R.); amypc82@gmail.com (W.-C.W.)

³ Department of Chemistry, Massachusetts Institute of Technology, Cambridge, MA 02139, USA; awanishmphil@gmail.com

⁴ School of Pharmacy, China Medical University, 91, Hsueh-Shih Road, Taichung 40402, Taiwan; hylin@mail.cmu.edu.tw

* Correspondence: changcj@fcuoa.fcu.edu.tw; Tel.: +886-4-2451-7250 (ext. 3678)

† These authors contributed equally to this work.

Academic Editor: Martin Kröger

Received: 3 May 2016; Accepted: 13 June 2016; Published: 18 June 2016

Abstract: Knowledge of the interactions between polymer and protein is very important to fabricate the potential materials for many bio-related applications. In this regard, the present work investigated the effect of copolymers on the conformation and thermal stability of bovine serum albumin (BSA) with the aid of biophysical techniques such as fluorescence spectroscopy, circular dichroism (CD) spectroscopy and differential scanning calorimetry (DSC). In comparison with that of copolymer PGA-1.5, our fluorescence spectroscopy results reveal that the copolymer PGA-1, which has a lower PEGMA/AA ratio, shows greater influence on the conformation of BSA. Copolymers induced unfolding of the polypeptide chain of BSA, which was confirmed from the loss in the negative ellipticity of CD spectra. DSC results showed that the addition of PGA-1 and PGA-1.5 (0.05% (*w/v*)) decreased the transition temperature by 14.8 and 11.5 °C, respectively). The results from the present study on the behavior of protein in response to changes in the chemical composition of synthetic polymers are significant for various biological applications such as enzyme immobilization, protein separations, sensor development and stimuli-responsive systems.

Keywords: protein; responsive polymer; thermal stability; folding; unfolding; biomedical applications

1. Introduction

Synthetic polymers, particularly stimuli responsive polymers, have received extensive attention and opened a broad field of potential applications in bioimaging, drug delivery, tissue engineering and bioactive surfaces [1–5], due to their extraordinary response to changes in temperature, pH, ionic strength and enzymes [6–14]. Among hundreds of polymers, poly(*N*-isopropylacrylamide) (PNIPAM) and its derivatives have widely been applied in protein science [15–18]. Schachschal *et al.* [19] reported that the activity of laccase was improved by immobilization in PNIPAM microgel. The stability of horseradish peroxidase (HRP) was improved upon incorporation in PNIPAM-based hydrogels [17]. Generally speaking, these proteins interacted with the polymeric materials through hydrophobic interactions, electrostatic interactions and hydrogen bonds [20].

Despite the abundant literature on protein-polymer interactions, a large portion of the literature is confined to the study of the behavior of immobilized proteins [17,19,21–23]. Such observations often lead to an intuitive conclusion that the interactions of polymers with proteins are either very weak or almost zero [24]. Moreover, the behavior of proteins on these surfaces is significantly governed by the surface properties of the polymer and thereby, study of the behavior of proteins on polymeric surfaces does not truly reflect the behavior of a protein in solution. In this regard, the study of the behavior of proteins in solution in the presence of polymers is desirable and important to extend the applications of polymers. Therefore, we aim in this study to explore the behavior of a model protein, bovine serum albumin (BSA), in the presence of thermoresponsive PNIPAM-based polymers in aqueous medium with the aid of biophysical techniques and simulation studies.

BSA is the most abundant globular protein in the plasma. This protein is commonly used as a model protein due to its medicinal importance, low cost, ready availability, stability, water solubility and structural similarity with human serum albumin (HSA) [25,26]. Various endogenous and exogenous ligands are transported by BSA [27]. Structurally, BSA is a single chain of 582 amino acids, non-glycoprotein, cross-linked with 17 cysteine residues [28]. Three types of intrinsic fluorophores are present in BSA: tryptophan (Trp), tyrosine (Tyr) and phenylalanine (Phe) [29]. There are two tryptophan residues in BSA: Trp-212 is located in a hydrophobic binding pocket, and Trp-134 on the surface of molecule [30]. The BSA molecule is made up of three homologous domains (I, II, III) that can be divided into nine loops (L1–L9) by 17 disulphide bonds. Each domain in turn is the product of two subdomains (IA, IB, etc.) [31]. Trp-134 is in the first domain, and Trp-212 is in the second domain. All these structural features make BSA one of the best models to understand the physicochemical basis of polymer-protein interactions.

Herein, we prepared copolymers, (poly(*N*-isopropylacrylamide-co-ethylene glycol methacrylate-co-acrylic acid)-1 (P(NIPAM-co-PEGMA-AA)-1; abbreviated as PGA-1) and poly(*N*-isopropylacrylamide-co-ethylene glycol methacrylate-co-acrylic acid)-1.5 (P(NIPAM-co-PEGMA-AA)-1.5; abbreviated as PGA-1.5)) by keeping the mole ratio of *N*-isopropyl acrylamide (NIPAM) unchanged, while changing the mole ratios of polyethyleneglycol methacrylate (PEGMA) and acrylic acid (AA). Polymers based on these components have been explored for a wide range of applications in multiple fields. For instance, poly(*N*-isopropylacrylamide) (PNIPAM) is a well-known environmentally sensitive polymer, which shows lower critical solution temperature (LCST) behavior in water [32]. This characteristic behavior of PNIPAM aqueous systems has been studied for use in a number of biomedical fields, such as drug delivery systems [33,34], tissue engineering [35], cell therapy [36] and so on. Being water soluble, nontoxic and non-immunogenic in nature, PEGMA is frequently used for introduction into a polymer structure. Such introduction offers several biological advantages including a prolonged lifetime in the bloodstream due to decreased uptake of PEG-conjugates by the reticuloendothelial system of the body, thereby reducing the toxicity and improving the biocompatibility of the PEG-containing polymer [37]. Further, it was shown that poly(acrylic acid)-based drug carriers were successfully applied in delivering bioadhesive drugs [38]. All these excellent applications inspired us to prepare copolymers consisting of NIPAM, PEGMA and AA. Therefore, we believe that the copolymers based on these monomers are suitable model systems to understand the behavior of biomolecules in the presence of polymers. Further, the present study also presents the behavior of BSA in response to changes in the chemical composition of these responsive polymers. Molecular docking simulation studies provided information about the type and strength of the copolymer-protein interactions. Since the study of the behavior of BSA in the presence of responsive polymers plays a key role in determination of the polymer's biocompatibility for various biomedical applications and thus helps in the rational design of effective therapeutic carriers, the present results may pave the way to construct PNIPAM-based biomedical devices.

2. Experimental Section

2.1. Materials

The monomers *N*-isopropylacrylamide (NIPAM), and acrylic acid (AA) were provided by Acros (Fairlawn, NJ, USA). *N,N,N',N'*-tetramethylethylenediamine (TEMED), ammonium persulfate (APS), *N,N'*-methylenebisacrylamide (MBAA) (cross-linker), and poly ethylene glycol methacrylate (PEGMA, $M_n = 360$) were obtained from the Aldrich Chemical Co. (St. Louis, MO, USA). BSA was obtained from Sigma-Aldrich (St. Louis, MO, USA). Deionized (DI) water with a resistivity of $18.2 \text{ M}\Omega \cdot \text{cm}$ was obtained from Roda purification system (Te Chen Shen Engineering Co., Ltd., Taichung, Taiwan) and used for all sample preparation. All the chemicals were used as received. All the prepared hydrogel samples were lyophilized using a freeze-dryer before the measurements.

2.2. Synthesis of P(NIPAM-co-PEGMA-co-AA) Copolymers

The procedure for the synthesis of these copolymers can be found elsewhere [39]. P(NIPAM-co-PEGMA-co-AA) copolymers were prepared by following the procedure described here. Initially, PEGMA was mixed with AA thoroughly. Subsequently, the resultant solution was transferred into a three-necked round-bottom flask containing NIPAM and MBAA in phosphate buffered saline. The reaction mixture was subjected to stirring for 30 min with continuous N_2 gas purging. Finally, to this solution, TEMED and APS were added and reacted for 19 h at room temperature under nitrogen atmosphere. The feed ratio of $[\text{NIPAM}]/[\text{PEGMA}]/[\text{AA}]/[\text{APS}]/[\text{MBAA}]$ in P(NIPAM-co-PEGMA-co-AA)-1 is $9.54 \times 10^{-5}/1.87 \times 10^{-5}/1.87 \times 10^{-5}/3.94 \times 10^{-7}/2.36 \times 10^{-7} \text{ mol} \cdot \text{L}^{-1}$, respectively, and the feed ratio of $[\text{NIPAM}]/[\text{PEGMA}]/[\text{AA}]/[\text{APS}]/[\text{MBAA}]$ in P(NIPAM-co-PEGMA-co-AA)-1.5 is $9.54 \times 10^{-5}/2.25 \times 10^{-5}/1.5 \times 10^{-5}/3.94 \times 10^{-7}/2.36 \times 10^{-7} \text{ mol} \cdot \text{L}^{-1}$, respectively. The codes 1 and 1.5 indicate the mole ratios of PEGMA to AA in the copolymer. All the hydrogels were freeze-dried before use. The results for characterization and phase transition of these polymers can be found in our recent work [39]. In our previous work, these polymers were abbreviated as PGA-4 and PGA-7 based on the weight fractions of PEGMA and AA. However, in the present study, the names have been changed from PGA-4 and PGA-7 to PGA-1 and PGA-1.5, respectively, for the sake of convenience.

2.3. Sample Preparation

Aqueous solutions of the copolymers at various concentrations (0.05, 0.1 and 0.5% *wt/vol*) were prepared for all the measurements by following the procedure, with minimal modifications, reported in previous literature [40]. First, an appropriate amount of freeze-dried copolymer was mechanically ground. This mechanically ground polymer sample was dissolved in a sufficient amount of DI water to obtain the required polymer concentrations (0.05, 0.1 and 0.5% *wt/vol*). The solution was rigorously stirred for four days. After stirring, the samples were additionally sonicated for 30 min. Finally, to this solution, the required amount (0.5 mg/mL) of BSA was added.

2.4. Fluorescence Intensity Measurements

Fluorescence intensities of the samples were obtained using a Hitachi F-7000 fluorescence spectrophotometer (Tokyo, Japan) with xenon lamp (150 W) as the light source. All the measurements were done at room temperature and atmospheric pressure. The emission spectra were recorded with a slit width of 2.5/2.5 nm and a PMT voltage of 720 V. The scan speed was $1200 \text{ nm} \cdot \text{min}^{-1}$. Tryptophan (Trp) of BSA was selected as an intrinsic fluorescent probe and excited at the wavelength (λ_{exc}) of $\sim 285 \text{ nm}$ for the emission spectra.

2.5. Circular Dichroism (CD) Spectroscopy

Circular dichroism spectroscopy (Jasco J-715 spectropolarimeter, Tokyo, Japan) was used to record the structural changes of BSA in aqueous solution induced by the addition of copolymers. The CD spectrum was measured in the wavelength ranging from 190 to 250 nm, with a 0.2 nm step resolution, a 50 nm/min speed, a 2 s response time, and a 1 nm bandwidth. Each sample spectrum was obtained by averaging six spectra.

2.6. Differential Scanning Calorimetry (DSC)

All the calorimetric measurements were performed on a nano DSC III (TA instruments, Wood Dale, IL, USA) and the data were used to measure the melting temperature (T_m) of BSA in the absence and presence of polymers. Before performing the experiment, the instrument was calibrated with pure water. A certain amount of bubble-free solution was placed into a sample cell, while the reference cell was filled with an appropriate blank sample of the same solvent media without BSA, then capped, and sealed using a press. The cells were allowed to stabilize at 20 °C and then heated to 75 °C with a heating rate of 2.0 °C/min. Enthalpy change (ΔH_{cal}) and the T_m of the sample were determined with the aid of software, which accompanied the instrument.

2.7. Molecular Docking (MD) Simulations

The molecular docking simulations to understand the interactions between the BSA (PDB No.: 4F5S) and copolymer was performed using the CLC Drug Discovery Workbench (trial version-2.5, Aarhus, Denmark) downloaded from CLC Bio website [41], with the default parameter settings [42]. Energy minimization for the BSA structure was performed using the YASARA SERVER [43]. This server performs an energy minimization using the YASARA force field [44]. The structure of the copolymer was created by using an equal number of monomers units, with the help of Chem Biodraw Ultra. The geometry of the polymer was optimized using Chem Biodraw Ultra with the default settings and the structure was saved in MDL Molfile (*.mol) format for further docking studies. The copolymer was transformed to a ligand before performing the docking studies. According to the developers, the docking score used in the Drug Discovery Workbench is the PLANTS_{PLP} score [45]. The score has a good balance between accuracy and evaluation time. The score mimics the potential energy change when the protein and ligand come together. The structural visualization for the interactions between BSA and the copolymer was performed using the CLC Drug Discovery Workbench.

3. Results and Discussion

In order to gain more insight into the behavior of BSA in the presence of P(NIPAM-co-PEGMA-co-AA) copolymers, the influence of the polymers on the fluorescence spectrum of the protein was investigated (Figure 1). The fluorescence measurements provide the information regarding the molecular environment of the chromophore. BSA contains intrinsic fluorescence fluorophores, tryptophan (Trp), and 18 tyrosine residues that are responsible for its fluorescence emission. Trp is located in subdomain IIA within a hydrophobic pocket, whereas tyrosines are distributed along the whole polypeptide chain. These fluorophores can be excited at the wavelength (λ_{exc}) of ~285 nm; however most of the fluorescence attributed to Trp because of the efficient resonance energy transfer (RET) from tyrosine to tryptophan [46]. Since the Trp fluorophore can be excited at the wavelength (λ_{exc}) of ~285 nm, the excitation of all other amino acids in the protein can be avoided as these absorb at shorter wavelength [20]. The fluorescence of Trp in the protein is sensitive to environmental changes such as polarizability [47], and thus it can be used as an optical probe to analyze the effect of co-solute on the conformational changes of the protein [48]. The changes in the fluorescence parameters such as maximum emission wavelength (λ_{emi}) and intensity (I_{max}) can be related to the conformational changes of the protein [49].

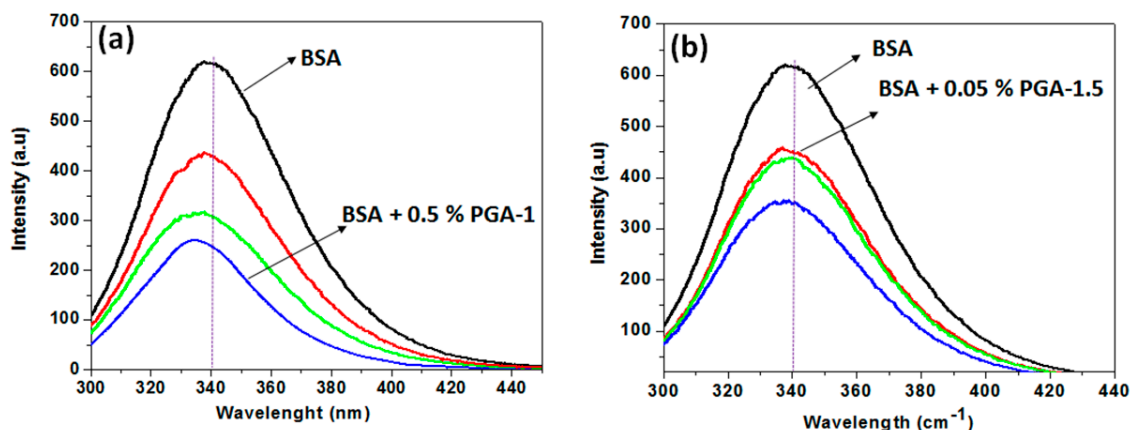
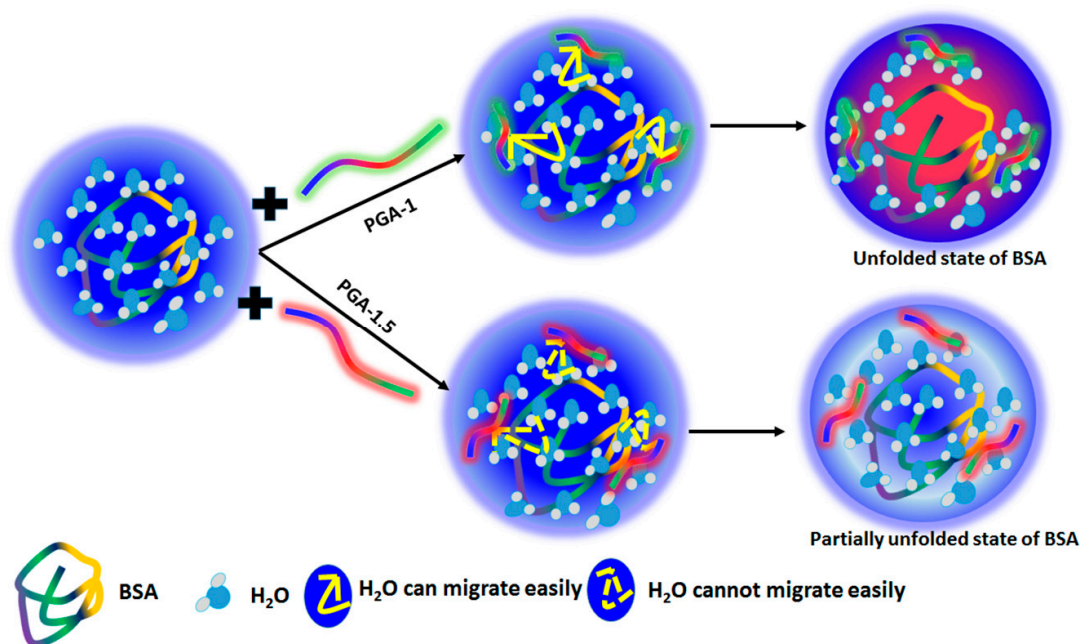


Figure 1. Fluorescence intensities of BSA in the absence and presence of PGA-1 (a); and PGA-1.5 (b) at various concentrations. The concentrations of polymers are 0.05% (red color line), 0.1% (green color line), and 0.5% (blue color line). The excitation wavelength of Trp is 295 nm.

Figure 1 shows the fluorescence spectra of BSA in the absence and presence of copolymers (PGA-1 & PGA-1.5) in water, at atmospheric temperature, with different concentrations of the copolymers. As shown in Figure 1, the maximum fluorescence intensity (I_{\max}) (619.5 a.u.) of BSA was observed at ~ 341 nm in the absence of the polymers, characteristic of Trp, indicating that this residue is relatively buried inside the BSA [50]. The addition of both the polymers resulted in substantial decrease of I_{\max} of BSA. However, the effect of PGA-1.5 (Figure 1b) on the intrinsic fluorescence intensity of BSA was less pronounced as compared to that in the presence of PGA-1 (Figure 1a). These results suggest that the ability of PGA-1 to unfold BSA was stronger, and thus this polymer strongly quenches the fluorescence of BSA. It is reported that the folded conformation of BSA in water is attributed to the formation of a water shell around the BSA [49]. In the present study, the equal distribution of monomers, PEGMA and AA, cause PGA-1 to be more hydrophilic [39], and thereby this polymer can easily alter the hydration shell around the BSA. Moreover, the optimum amount of PEGMA in PGA-1 can increase the bulkiness of the backbone of polymer, and thereby, restricts the flexibility of the entire copolymer system and results in more hydrophilicity by hindering the formation of the intramolecular hydrogen bonds [39,51]. Therefore, the behavior (flexible/stiff) of the polymer is the result of intermolecular hydrogen bonds. Moreover, strong intramolecular hydrogen bonding at certain composition makes the polymer less hydrophilic, despite the higher content of the hydrophilic monomer [51]. Therefore, it is very important to fabricate the polymer with optimal chemical composition.

For a more intuitive understanding of the unfolding mechanism of BSA in the presence of copolymers (represented by the three color segments (blue, red and green, and these three colors represent three monomer units in the copolymers), a schematic illustration is presented in Scheme 1. As illustrated in the scheme, BSA is fully hydrated in the absence of the polymers. However, the addition of PGA-1 (represented by the green line in Scheme 1) to the protein aqueous solution results in competition for water molecules between the polymer and protein. Due to the higher hydrophilic nature of PGA-1, the water molecules from the surface of the protein can migrate easily to this polymer and thus make BSA unfold easily (represented by the red area in Scheme 1). On the other hand, despite the unfolding of BSA in the presence of PGA-1.5 (represented by the red line in Scheme 1), the extent of unfolding seems to be smaller when compared that in the presence of PGA-1. Due to the higher hydrophobic nature, PGA-1.5 cannot attract water molecules easily from the hydration shell around the protein and lead to partial unfolding (represented by light blue area in Scheme 1). Therefore, the higher fluorescence intensity of BSA was observed in the presence of PGA-1.5 (Figure 1b). The enzyme activity mainly depends on the volume of the hydration shell around the protein, but not on the volume of bulk water [52]. A similar decrease in the I_{\max} of Trp was observed when exposed to the water molecules in the presence of additives [53,54]. These results indicate that the conformation of BSA was significantly

altered by the addition of both polymers. Moreover, the I_{\max} of BSA decreased with an increase in the concentration of both the copolymers PGA-1 and PGA-1.5 (Figure 1a,b). For instance, the I_{\max} of BSA was 451 a.u. in the presence of PGA-1.5 at a concentration of 0.05% (w/v), while I_{\max} was found to be 356 a.u. at a concentration of 0.5% (w/v) (Figure 1b). On the other hand, the I_{\max} of BSA was 435 a.u. in the presence of PGA-1 at a concentration of 0.05% (w/v), while I_{\max} was found to be 264 a.u. at a concentration of 0.5% (w/v). The decrease in I_{\max} by increasing the concentration of the polymer can be regarded to the maximum change in the conformation of the protein. It is worth mentioning here that the 0.05% (w/v) PGA-1.5 was able to quench the fluorescence intensity by altering the hydration layer around the protein. However, the fluorescence intensity was not further quenched significantly with an increase in the concentration of PGA-1.5 from 0.05% ($I_{\max} = 451$ a.u.) to 0.1% (w/v) ($I_{\max} = 437$ a.u.) (Figure 1b). This can be attributed to the higher hydrophobic nature of PGA-1.5. Being more hydrophobic, PGA-1.5 cannot attract the water molecule in the close vicinity of the protein surface at a concentration of 0.1% (w/v). However, the water molecules from the close vicinity of protein surface can migrate by the addition of a higher amount of polymer as evidenced from the quenching of fluorescence by the addition of 0.5% (w/v) PGA-1.5 (Figure 1b). A similar type of decrease was observed in the I_{\max} of serum protein with the addition of the copolymers [37].



Scheme 1. Schematic demonstration of the unfolding mechanism of BSA in the presence of PGA-1 and PGA-1.5.

Further, Figure 1a indicates a shift in the λ_{emi} of BSA towards a shorter wavelength (hypsochromic shift) with the addition of the polymers. For instance, in the absence of copolymers, BSA has λ_{emi} at ~ 340 nm. However, with the addition of PGA-1, the λ_{emi} shifted to lower wavelengths (338, 337 and 334 for 0.05, 0.1 and 0.5 % (w/v), respectively). On the other hand, despite the blue shift in λ_{emi} of BSA by the addition of PGA-1.5, the extent of the shift was less significant than with PGA-1. For instance, the λ_{emi} shifted to ~ 337 nm by the addition of 0.5% (w/v) PGA-1.5. This blue shift in λ_{emi} indicated that the tryptophan residue experienced a more hydrophobic (less polar) environment in the presence of the polymers [55]. Azegami *et al.* [55] reported a hypsochromic shift of λ_{emi} of serum protein upon interaction with high molecular weight PEG. They explained this hypsochromic shift of λ_{emi} on the basis of protein-protein complex formation induced by large PEG chains. The hypsochromic shift in the λ_{emi} of BSA observed upon the complexation with the copolymers can

be explained on the basis of a similar phenomenon where the PEGMA segments in the copolymers induced a protein-protein interaction. These BSA molecules may interact with themselves or with nearby PEGMA chains present in the copolymer, which can result in the hypsochromic shift of emission maximum as shown in Figure 1. The presence of PEGMA in the copolymers at higher content resulted in higher hydrophobicity with respect to the PGA-1.5 and thus, this polymer is not that effective in perturbing the hydration layer as evidenced from Figure 1b. These results are consistent with the results of existing studies [37]. Further, Zhao *et al.* [56] reported that the fluorescence intensity of tryptophan buried inside BSA is much stronger when compared to that exposed to the water molecules in aqueous solution at the same concentration.

CD spectroscopy has been proved as a technique of choice to extract information regarding the secondary structure of proteins and nucleic acids [57]. BSA exhibits two characteristic negative bands in the UV region at 208 and 220 nm, indicating an α -helical structure of the protein [53]. The negative band at 208 nm is due to the exciton splitting of the lowest peptide $\pi \rightarrow \pi^*$ transition, while the negative band at 220 nm is due to the peptide $n \rightarrow \pi^*$ transition [58].

Typical far-UV CD spectra of BSA in the absence and presence of PGA-1 and PGA-1.5 at different concentrations are presented in Figure 2. BSA showed a typical CD signature with a high alpha helical content with considerable negative ellipticity at ~ 208 and ~ 220 nm in the far UV range in the absence of copolymers as shown in Figure 2. Neither of the polymers showed the CD signal in the range of 190–250 nm, and thus the observed CD was solely due to the peptide bonds of the protein. The negative bands at ~ 208 and ~ 220 nm were found to be collapsed by the addition of PGA-1 (Figure 2a) and PGA-1.5 (Figure 2b). These results indicated that the intramolecular forces responsible for maintaining the secondary structure were altered in the presence of these polymers. Such changes can be viewed from the alterations in the circular dichroism (CD) spectrum of the protein as presented in Figure 2. With an increase in copolymer concentration, a further reduction in the magnitude of negative ellipticity of the CD bands was observed. However, in the presence of the PGA-1.5 copolymer (Figure 2b), the loss of magnitude of negative ellipticity was smaller when compared to PGA-1 (Figure 2a). This is in agreement with the fluorescence quenching data presented earlier. A reduction in the magnitude of negative ellipticity of the CD bands of BSA occurred to a greater extent in the presence of PGA-1, as was pointed out previously in the quenching experiments, *i.e.*, as PGA-1 was added, it easily altered the hydration shell around BSA, and thus led to BSA undergoing the unfolding process easily. The polymer-induced alterations in the peaks at 208 and 220 nm suggested that the polymers were effective in initiating partial unfolding of the protein chain. Similar partial unfolding behaviors of the protein chains due to the presence of ionic liquids and dendrimers in the aqueous protein solutions have also been reported [59,60].

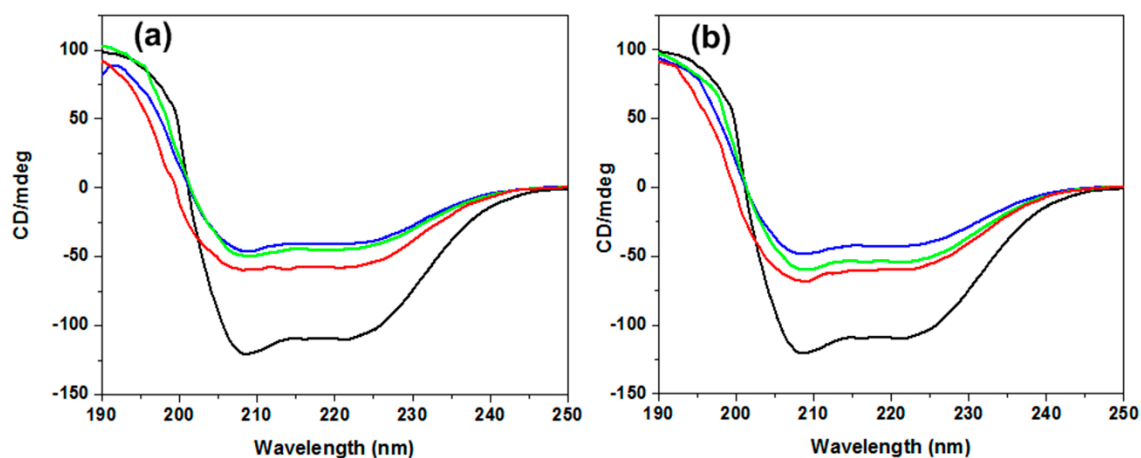


Figure 2. Far-UV CD spectra of BSA (black line) and BSA in the presence of PGA-1 (a); and PGA-1.5 (b). The concentrations of polymers are 0.05% (red line), 0.1% (green line), and 0.5% (blue line).

The thermal unfolding of the serum albumin protein proceeds in multiple steps; [61] native (N) \rightarrow extended (E) \rightarrow unfolded (U). In the extended form (E) (at ≤ 55 °C), despite the displacement of domains I and II, the protein almost maintains its native conformation, whereas in the unfolded state (U), domain II starts to melt, disrupting the secondary and tertiary structure of the protein. Moreover, the N \rightarrow E transition is reversible. However, for the E \rightarrow U transition, the native state cannot be retrieved upon decreasing the temperature. The change in the T_m values of the BSA upon the addition of the copolymers was obtained from DSC thermograms (Figure 3). The T_m was determined as the highest point of the heat flow in the DSC thermograms. As shown in Figure 3, BSA has reduced T_m values in the presence of copolymers. For instance, the T_m of BSA decreased from 66.7 °C (in the absence of copolymers) to 51.9 °C (0.05% w/v), 48.1 °C (0.05% w/v) and 39.6 °C (0.05% w/v) in the presence of PGA-1. This decrease in the T_m of BSA upon the addition of polymers was attributed to the perturbation of the hydration layer around the BSA surface. However, the extent of the decrease in T_m was greater in the presence of PGA-1 at a given concentration. For instance, at 0.05% (w/v) PGA-1 (Figure 3a), T_m of BSA decreased by 14.8 °C, whereas the T_m decreased by 11.5 °C in the presence of PGA-1.5 (Figure 3b). This result implied that the thermal stability of BSA decreased, and both copolymers acted as structure destabilizers. However, PGA-1 can be considered as a relatively stronger destabilizer as it shifts T_m to a greater extent (Figure 3a). The thermal stability of the folded protein is mainly governed by the ordering of water molecules around the hydrophobic groups of the protein [62]. The loss of the hydration layer around the peptide of BSA resulted from the preferential interactions between the polymer and water molecules. Moreover, it is worth mentioning that each sample exhibited the broad peak after the T_m value in the DSC thermogram as shown in the figure, indicating the aggregation of the BSA-copolymer complex at higher temperatures.

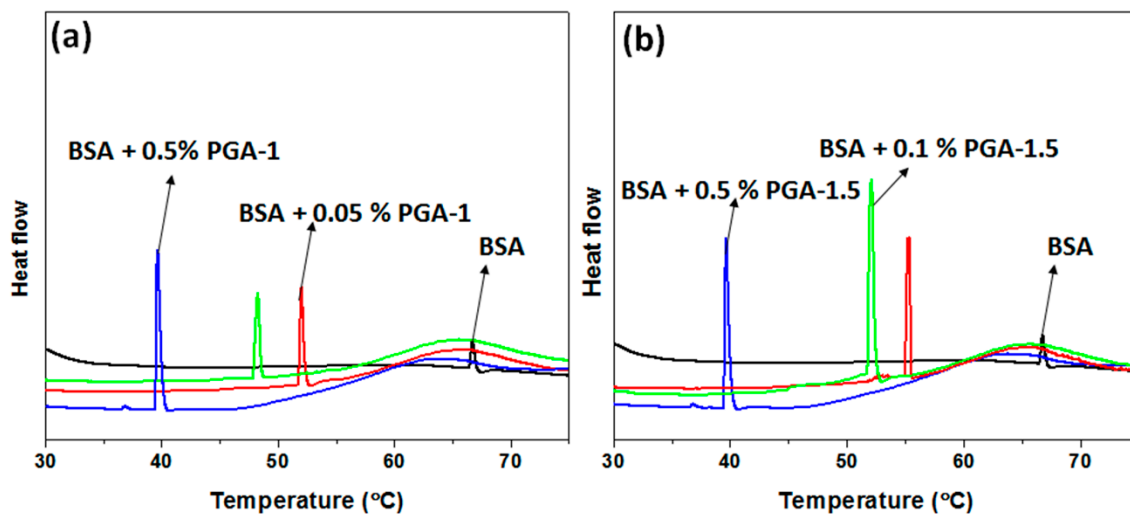


Figure 3. DSC thermograms of BSA in the absence and presence of PGA-1 (a) and PGA-1.5 (b) at various concentrations. The concentrations of the polymers are 0.05% (red line), 0.1% (green line), and 0.5% (blue line). T_m represents the highest point of relative heat.

The differences in the behavior of the T_m of BSA in response to the PGA-1 and PGA-1.5 copolymers at the same concentration can be attributed to the differences in the PEGMA/AA ratios of these copolymers. The contents of PEGMA and AA are the same in the PGA-1 copolymer. Such equal distribution of monomers makes the polymer relatively more hydrophilic and thus PGA-1 can easily perturb the hydration layer around the protein. In contrast to this, with further enhancement of PEGMA content as in PGA-1.5 copolymer, the resulted copolymer becomes relatively less hydrophilic. Due to this relatively less hydrophilic nature, PGA-1.5 needs more energy to perturb the hydration layer around the proteins and thus T_m was observed at higher temperatures. The relative hydrophilic natures of these copolymers can be monitored from their lower critical solution temperatures (LCST)

(LCST values of these copolymers were measured from the DSC thermograms) as reported in our previous work [32]. These results reveal that the distribution of monomers plays a significant role in governing the hydrophilic/hydrophobic nature of the copolymer, and consequently their effect on the behavior of proteins. Further, there are reports where the distribution of monomers controlled the hydrophilic/hydrophobic properties of the resulted copolymer [63,64]. Further, the unfolding enthalpy (ΔH_{cal}) of BSA ($253 \text{ KJ} \cdot \text{mol}^{-1}$) decreased upon addition of PGA-1 (198, 145 and $140 \text{ KJ} \cdot \text{mol}^{-1}$ for 0.05%, 0.1% and 0.5% (w/v), respectively) and PGA-1.5 (212, 189 and $160 \text{ KJ} \cdot \text{mol}^{-1}$ for 0.05%, 0.1% and 0.5% (w/v), respectively) as shown in Figure 4 and strongly consistent with the T_m values. Considering the fluorescence, CD and DSC results, we believe that both polymers can change conformation. In order to obtain more insight into the molecular level interactions, we performed molecular docking simulations.

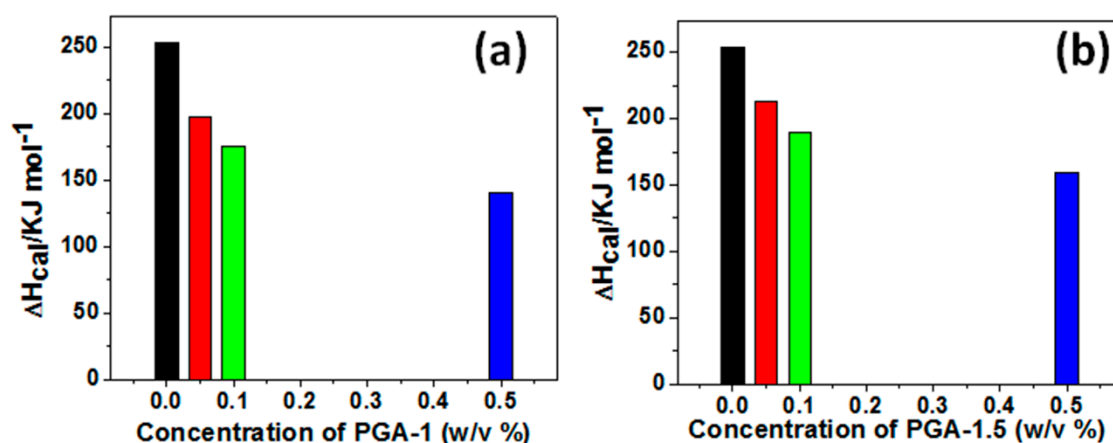


Figure 4. The changes in ΔH_{cal} of BSA upon addition of PGA-1 (a); and PGA-1.5 (b) at various concentrations.

Molecular docking simulations can be used as a complementary tool to understand the protein-ligand interactions at a molecular level. The molecular docking simulation was performed using the CLC Drug Discovery Workbench. The first step in molecular docking is to identify the most probable and potential binding pockets within the protein structure. Under the default settings, CLC identifies a number of binding pockets lying within the range of 20 to 632.83 \AA in the structure of BSA. Therefore, we have confined our search for the binding pockets that are greater than 100 \AA . Moreover, analysis of several protein-ligand structures from the Protein Data Bank (PDB) revealed that most of the binding sites were the largest pockets found on the protein [65].

As presented in Figure 5a (the green areas), three potential binding sites were identified over the surface of the BSA with the molecular dimension of 632.83 , 422.40 and 127.49 \AA . On the other hand, in order to compare the magnitude of interaction of the copolymer with the BSA, we have individually docked the monomers of the copolymer, such as NIPAM, AA, and PEGMA, with the BSA, and the H-bond score is presented in Table 1. Apparently, if arranged in the order of increasing hydrogen bonding score, the order is NIPAM < PEGMA < acrylic acid < copolymer. The docking result shows that NIPAM interacts only with the Tyr 137 residue (Figure 5b), whereas, PEGMA interacts with the Leu 189 and Set 192 residues (Figure 5c). On the other hand, AA shows hydrogen bonding with Arg 144, Leu 112 and Asp 111 residues (Figure 5d). The most promising result is with the copolymer that interacts with Ser 109, Arg 144, Arg 185, Glu 424, Arg 427 and Ser 428 amino acid residues within the binding pocket (Figure 5e). The possible interacting model for the copolymer involved in the interaction is depicted in Figure 5f, for the largest binding pocket of 632.83 \AA .

The difference in the hydrogen bonding for the NIPAM, PEGMA, AA and the copolymer can also be accounted for the molecular structure. It is a well-known fact that the docking process follows the lock and key mechanism and thus, if the properties (such as size, shape and charge, *etc.*) of the

ligands match with the properties of binding pocket a, high docking score can be achieved. A similar phenomenon was observed in the case of NIPAM, PEGMA, AA and the copolymer. The size of the copolymer is obviously higher as compared to the rest of its components. This indicates that the copolymer fits much better into the binding pockets of BSA during docking and hence, we observe the highest docking score for the copolymer in all of the three predicted binding pockets of BSA. Due to the perfect match in the size of the copolymer with the binding pocket, the surrounding amino acids come close enough to form strong hydrogen bonding with the polymer. Hence, due to the preferable interaction of the copolymer with the protein surface, the solvation structure of water molecules around the binding pockets are displaced and hence, the structure of the protein is disturbed. Moreover, the intermolecular hydrogen bonding interaction of amino acid residues with the copolymer decreased the hydrophobicity of the system. Therefore, we observed quenching in the fluorescence as well as thermal instability of BSA in the presence of the copolymer.

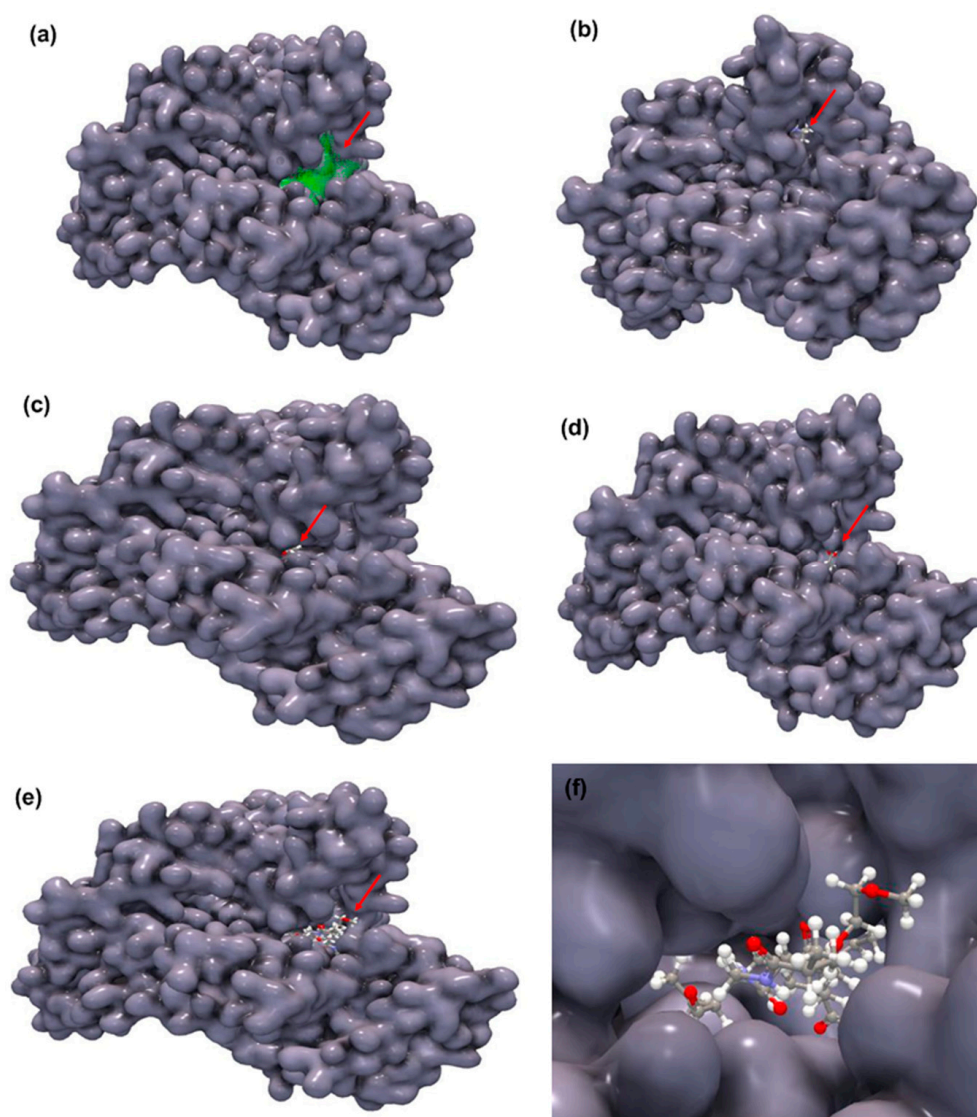


Figure 5. Molecular docking snapshots of the potential binding sites of BSA (a); interactions of NIPAM with BSA (b); interactions of PEGMA with BSA (c); interactions of AA with BSA (d); interactions of copolymer with BSA (e); and the magnified images for interactions of the copolymer with the largest binding pocket of the BSA (f). The red arrow indicates the position of the monomer or copolymer in the protein.

Table 1. Docking score and hydrogen bond (H-bond) score for the interaction of the copolymer, PEGMA, NIPAM and AA with the best selected docking position of BSA.

Molecular dimensions of the binding sites	Docking score	H-bond score
Copolymer		
632.83 Å	−61.86	−19.13
422.83 Å	−45.87	−14.57
127.49 Å	−59.78	−4.00
PEGMA		
632.83 Å	−27.44	−4.00
422.83 Å	−27.48	−8.00
127.49 Å	−31.39	−3.98
NIPAM		
632.83 Å	−23.99	−0.72
422.83 Å	−27.68	−4.00
127.49 Å	−28.78	0.00
AA		
632.83 Å	−22.91	−9.72
422.83 Å	−21.73	−11.62
127.49 Å	−20.50	−4.00

4. Conclusions

The applications of stimuli-responsive polymers as therapeutic carriers can be amplified by the comprehensive understanding of their influences on behaviors of biomolecules. In this context, the stability of the model protein, BSA, in the presence of PNIPAM based thermoresponsive copolymers with different PEGMA/AA ratios was evaluated in aqueous solution with the aid of experimental and docking studies. Our experimental and docking results showed that the chemical structure and composition of the constituted monomers of the polymers play a significant role in governing the behavior of the protein in aqueous solution. Molecular docking simulation revealed that the surrounding amino acids come close enough to form strong hydrogen bonding with the polymer because of the perfect match in the size of the copolymer with the binding pocket. Hence, due to the preferable interaction of the copolymer with the protein surface, the solvation structure of water molecules around the binding pockets is displaced and hence, the structure of the protein is perturbed. The thermal stability and secondary structure of BSA are greatly affected by PGA-1. The higher destabilizing ability of PGA-1 can be attributed to the relative higher hydrophilicity. PEGMA and AA are distributed equally in the PGA-1 copolymer. Such equal distribution of monomers makes the polymer relatively more hydrophilic and thus PGA-1 can easily perturb the hydration layer around the protein. The present results can pave the way for the correct selection of chemical structure and composition of monomers to prepare the stimuli responsive polymers that can be used for biomedical applications.

Acknowledgments: The authors are grateful for the financial support from Feng Chia University and the Taichung Veterans General Hospital under contract number TCVGH-FCU1048201. The authors appreciate the Precision Instrument Support Center of Feng Chia University for providing the measurement facilities.

Author Contributions: Shih-Rong Hsieh, P. Madhusudhana Reddy, and Chi-Jung Chang designed the experiments and wrote the paper; Wan-Chi Wu carried out the experiments; Awanish Kumar performed the molecular docking simulations. Hui-Yi Lin analyzed the circular dichroism data.

Conflicts of Interest: The authors declare no conflict of interest.

References

1. Van Rijn, P. Polymer directed protein assemblies. *Polymers* **2013**, *5*, 576–599. [[CrossRef](#)]
2. Seelbach, R.J.; Fransen, P.; Pulido, D.; D'Este, M.; Duttenhoefer, F.; Sauerbier, S.; Freiman, T.; Niemeyer, P.; Albericio, F.; Alini, M.; *et al.* Injectable hyaluronan hydrogels with peptide-binding dendrimers modulate the controlled release of BMP-2 and TGF- β 1. *Macromol. Biosci.* **2015**, *15*, 1035–1044. [[CrossRef](#)] [[PubMed](#)]
3. Kavitha, T.; Kim, J.O.; Jang, S.; Kim, D.P.; Kang, I.K.; Park, S.Y. Multifaceted thermoresponsive poly(*N*-vinylcaprolactam) coupled with carbon dots for biomedical applications. *Mater. Sci. Eng. C* **2016**, *61*, 492–498. [[CrossRef](#)] [[PubMed](#)]
4. Lakhari, H.; Okano, T.; Nurdin, N.; Luthi, C.; Descouts, P.; Muller, D.; Jozefonvicz, J. Temperature-responsive size-exclusion chromatography using poly(*N*-isopropylacrylamide) grafted silica. *Biochim. Biophys. Acta* **1998**, *1379*, 303–313. [[CrossRef](#)]
5. Tan, S.W.; Han, C.; Wang, H.J.; Liu, D.R.; Tu, K.H.; Jiang, H.L.; Zhang, M.H.; Wang, L.Q. Preparation and characterization of thermo-sensitive mixed micelles and *in vitro* drug release. *Acta Polym. Sin.* **2011**, *11*, 1237–1243. [[CrossRef](#)]
6. Weber, C.; Hoogenboom, R.; Schubert, U.S. Temperature responsive bio-compatible polymers based on poly(ethylene oxide) and poly(2-oxazoline)s. *Prog. Polym. Sci.* **2012**, *37*, 686–714. [[CrossRef](#)]
7. Gil, E.S.; Hudson, S.M. Stimuli-responsive polymers and their bioconjugates. *Prog. Polym. Sci.* **2004**, *29*, 1173–1222. [[CrossRef](#)]
8. Chen, J.K.; Chang, C.J. Fabrications and applications of stimulus-responsive polymer films and patterns on surfaces: A review. *Materials* **2014**, *7*, 805–875. [[CrossRef](#)]
9. Schattling, P.; Jochum, F.D.; Theato, P. Multi-stimuli responsive polymers—The all-in-one talents. *Polym. Chem.* **2014**, *5*, 25–36. [[CrossRef](#)]
10. Zhang, Q.; Vanparijs, N.; Louage, B.; De Geest, B.G.; Hoogenboom, R. Dual pH- and temperature-responsive RAFT-based block co-polymer micelles and polymer-protein conjugates with transient solubility. *Polym. Chem.* **2014**, *5*, 1140–1144. [[CrossRef](#)]
11. You, S.; Cai, Q.; Müllen, K.; Yang, W.; Yin, M. pH-sensitive unimolecular fluorescent polymeric micelles: From volume phase transition to optical response. *Chem. Commun.* **2014**, *50*, 823–825. [[CrossRef](#)] [[PubMed](#)]
12. Chang, C.J.; Reddy, P.M.; Hsieh, S.R.; Huang, H.C. Influence of imidazolium based green solvents on volume phase transition temperature of crosslinked poly(*N*-isopropylacrylamide-co-acrylic acid) hydrogel. *Soft Matter* **2015**, *11*, 785–792. [[CrossRef](#)] [[PubMed](#)]
13. Umapathi, R.; Reddy, P.M.; Kumar, A.; Venkatesu, P.; Chang, C.J. The biological stimuli for governing the phase transition temperature of the “smart” polymer PNIPAM in water. *Colloids Surf. B* **2015**, *135*, 588–595. [[CrossRef](#)] [[PubMed](#)]
14. Hiruta, Y.; Nagumo, Y.; Suzuki, Y.; Funatsu, T.; Ishikawa, Y.; Kanazawa, H. The effects of anionic electrolytes and human serum albumin on the LCST of poly(*N*-isopropylacrylamide)-based temperature-responsive copolymers. *Colloids Surf. B* **2015**, *132*, 299–304. [[CrossRef](#)] [[PubMed](#)]
15. Hamerska-Dudra, A.; Bryjak, J.; Trochimczuk, A.W. Immobilization of glucoamylase and trypsin on crosslinked thermosensitive carriers. *Enzym. Microb. Technol.* **2007**, *41*, 197–204. [[CrossRef](#)]
16. Hamerska-Dudra, A.; Bryjak, J.; Trochimczuk, A.W. Novel method of enzymes stabilization on crosslinked thermosensitive carriers. *Enzym. Microb. Technol.* **2006**, *38*, 921–925. [[CrossRef](#)]
17. Zhao, Q.; Sun, J.; Ren, H.; Zhou, Q.; Lin, Q. Horseradish peroxidase immobilized in macroporous hydrogel for acrylamide polymerization. *J. Polym. Sci. A Polym. Chem.* **2008**, *46*, 2222–2232. [[CrossRef](#)]
18. Miletić, N.; Vuković, Z.; Nastasović, A.; Loos, K. Effect of *Candida antarctica* Lipase B immobilization on the porous structure of the carrier. *Macromol. Biosci.* **2011**, *11*, 1537–1543. [[CrossRef](#)] [[PubMed](#)]
19. Schachschaal, S.; Adler, H.J.; Pich, A.; Wetzel, S.; Matura, A.; van Pee, K.H. Encapsulation of enzymes in microgels by polymerization/cross-linking in aqueous droplets. *Colloid Polym. Sci.* **2011**, *289*, 693–698. [[CrossRef](#)]
20. Wu, J.; Zhao, C.; Hu, R.; Lin, W.; Wang, Q.; Zhao, J.; Bilinovich, S.M.; Leeper, T.C.; Li, L.; Cheung, H.M.; *et al.* Probing the weak interaction of proteins with neutral and zwitterionic antifouling polymers. *Acta Biomater.* **2014**, *10*, 751–760. [[CrossRef](#)] [[PubMed](#)]

21. Chen, Z.; Li, Q.; Chen, J.; Luo, R.; Maitz, M.F.; Huang, N. Immobilization of serum albumin and peptide aptamer for EPC on polydopamine coated titanium surface for enhanced in-situ self-endothelialization. *Mater. Sci. Eng. C* **2016**, *60*, 219–229. [[CrossRef](#)] [[PubMed](#)]
22. Derkus, B.; Emregul, K.C.; Emregul, E. Evaluation of protein immobilization capacity on various carbon nanotube embedded hydrogel biomaterials. *Mater. Sci. Eng. C* **2015**, *56*, 132–140. [[CrossRef](#)] [[PubMed](#)]
23. Ogorzalek, T.L.; Wei, S.; Liu, Y.; Wang, Q.; Brooks, C.L.; Chen, Z.; Marsh, E.N.G. Molecular-level insights into orientation-dependent changes in the thermal stability of enzymes covalently immobilized on surfaces. *Langmuir* **2015**, *31*, 6145–6153. [[CrossRef](#)] [[PubMed](#)]
24. Wu, J.; Zhao, C.; Lin, W.; Hu, R.; Wang, Q.; Chen, H.; Li, L.; Chen, S.; Zheng, J. Binding characteristics between polyethylene glycol (PEG) and proteins in aqueous solution. *J. Mater. Chem. B* **2014**, *2*, 2983–2992. [[CrossRef](#)]
25. Bharmoria, P.; Kumar, A. Thermodynamic investigations of protein's behaviour with ionic liquids in aqueous medium studied by isothermal titration calorimetry. *Biochim. Biophys. Acta* **2016**, *1860*, 1017–1025. [[CrossRef](#)] [[PubMed](#)]
26. Lomova, M.V.; Brichkina, A.I.; Kiryukhin, M.V.; Vasina, E.N.; Pavlov, A.M.; Gorin, D.A.; Sukhorukov, G.B.; Antipina, M.N. Multilayer capsules of bovine serum albumin and tannic acid for controlled release by enzymatic degradation. *ACS Appl. Mater. Interfaces* **2015**, *7*, 11732–11740. [[CrossRef](#)] [[PubMed](#)]
27. Anand, U.; Mukherjee, S. Binding, unfolding and refolding dynamics of serum albumins. *Biochim. Biophys. Acta* **2013**, *1830*, 5394–5404. [[CrossRef](#)] [[PubMed](#)]
28. Carter, D.C.; Ho, J.X. Structure of serum albumin. *Adv. Protein Chem.* **1994**, *45*, 153–203. [[PubMed](#)]
29. Peters, T. Serum albumin. *Adv. Protein Chem.* **1985**, *37*, 161–245. [[PubMed](#)]
30. Kragh-Hansen, U. Molecular aspects of ligand binding to serum albumin. *Pharmacol. Rev.* **1981**, *33*, 17–53. [[PubMed](#)]
31. Peters, T. *All about Albumin: Biochemistry, Genetics, and Medical Applications*; Academic Press: San Diego, CA, USA, 1995.
32. Schild, H.G. Poly(*N*-isopropylacrylamide): Experiment, theory and application. *Prog. Polym. Sci.* **1992**, *17*, 163–249. [[CrossRef](#)]
33. Wei, H.; Cheng, S.-X.; Zhang, X.-Z.; Zhuo, R.-X. Thermo-sensitive polymeric micelles based on poly(*N*-isopropylacrylamide) as drug carriers. *Prog. Polym. Sci.* **2009**, *34*, 893–910. [[CrossRef](#)]
34. Nakayama, M.; Okano, T.; Miyazaki, T.; Kohori, F.; Sakai, K.; Yokoyama, M. Molecular design of biodegradable polymeric micelles for temperature-responsive drug release. *J. Control. Release* **2006**, *115*, 46–56. [[CrossRef](#)] [[PubMed](#)]
35. Wu, J.-Y.; Liu, S.-Q.; Heng, P.W.-S.; Yang, Y.-Y. Evaluating proteins release from, and their interactions with, thermosensitive poly (*N*-isopropylacrylamide) hydrogels. *J. Control. Release* **2005**, *102*, 361–372. [[CrossRef](#)] [[PubMed](#)]
36. Cho, J.H.; Kim, S.-H.; Park, K.D.; Jung, M.C.; Yang, W.I.; Han, S.W.; Noh, J.Y.; Lee, J.W. Chondrogenic differentiation of human mesenchymal stem cells using a thermosensitive poly(*N*-isopropylacrylamide) and water-soluble chitosan copolymer. *Biomaterials* **2004**, *25*, 5743–5751. [[CrossRef](#)] [[PubMed](#)]
37. Banerjee, R.; Gupta, S.; Dey, D.; Maiti, S.; Dhara, D. Synthesis of PEG containing cationic block copolymers and their interaction with human serum albumin. *React. Funct. Polym.* **2014**, *74*, 81–89. [[CrossRef](#)]
38. Nho, Y.-C.; Park, J.-S.; Lim, Y.-M. Preparation of poly(acrylic acid) hydrogel by radiation crosslinking and its application for mucoadhesives. *Polymers* **2014**, *6*, 890–898. [[CrossRef](#)]
39. Reddy, P.M.; Chang, C.J.; Hsieh, S.; Huang, H.; Lee, M. Overview of the effect of monomers and green solvents on thermoresponsive copolymers: Phase transition temperature and surface properties. *RSC Adv.* **2015**, *5*, 86901–86909. [[CrossRef](#)]
40. Mikheeva, L.M.; Grinberg, N.V.; Mashkevich, A.Y.; Grinberg, V.Y.; Thanh, L.T.M.; Makhaeva, E.E.; Khokhlov, A.R. Microcalorimetric study of thermal cooperative transitions in poly(*N*-vinylcaprolactam) hydrogels. *Macromolecules* **1997**, *30*, 2693–2699. [[CrossRef](#)]
41. CLC Drug Discovery Workbench. Available online: <http://www.clcbio.com/products/clc-drug-discovery-workbench/> (accessed on 21 September 2015).
42. Krieger, E.; Joo, K.; Lee, J.; Lee, J.; Raman, S.; Thompson, J.; Tyka, M.; Baker, D.; Karplus, K. Improving physical realism, stereochemistry, and side-chain accuracy in homology modeling: Four approaches that performed well in CASP8. *Proteins* **2009**, *77*, 114–122. [[CrossRef](#)] [[PubMed](#)]

43. YASARA SERVER. Available online: <http://www.yasara.org/minimizationserver.htm> (accessed on 21 September 2015).
44. Korb, O.; Stützle, T.; Exner, T.E. Empirical scoring functions for advanced protein-ligand docking with plants. *J. Chem. Inf. Model.* **2009**, *49*, 84–96. [[CrossRef](#)] [[PubMed](#)]
45. CLC Drug Discovery Workbench—CLC Manuals. Available online: http://www.clcsupport.com/clcdrugdiscoveryworkbench/current/User_Manual.pdf (accessed on 21 September 2015).
46. Abou-Zied, O.K.; Al-Shihi, O.I.K. Characterization of subdomain IIA binding site of human serum albumin in its native, unfolded, and refolded states using small molecular probes. *J. Am. Chem. Soc.* **2008**, *130*, 10793–10801. [[CrossRef](#)] [[PubMed](#)]
47. Lakowicz, J.R. *Principles of Fluorescence Spectroscopy*; Lakowicz, J.R., Ed.; Springer: New York, NY, USA, 2006; pp. 529–575.
48. Deep, S.; Ahluwalia, J.C. Interaction of bovine serum albumin with anionic surfactants. *Phys. Chem. Chem. Phys.* **2001**, *3*, 4583–4591. [[CrossRef](#)]
49. Gupta, B.S.; Taha, M.; Lee, M.J. Buffers more than buffering agent: Introducing a new class of stabilizers for the protein BSA. *Phys. Chem. Chem. Phys.* **2015**, *17*, 1114–1133. [[CrossRef](#)] [[PubMed](#)]
50. Chaturvedi, S.K.; Ahmad, E.; Khan, J.M.; Alam, P.; Ishtikhar, M.; Khan, R.H. Elucidating the interaction of limonene with bovine serum albumin: a multi-technique approach. *Mol. Biosyst.* **2015**, *11*, 307–316. [[CrossRef](#)] [[PubMed](#)]
51. Keer, M.; Smirnovas, V.; Winter, R.; Richtering, W. Copolymer microgels from mono- and disubstituted acrylamides: Phase behavior and hydrogen bonds. *Macromolecules* **2008**, *41*, 6830–6836. [[CrossRef](#)]
52. Mittal, S.; Chowhan, R.K.; Singh, L.R. Macromolecular crowding: Macromolecules friend or foe. *Biochim. Biophys. Acta* **2015**, *1850*, 1822–1831. [[CrossRef](#)] [[PubMed](#)]
53. Huang, R.; Zhang, S.; Pan, L.; Li, J.; Liu, F.; Liu, H. Spectroscopic studies on the interactions between imidazolium chloride ionic liquids and bovine serum albumin. *Spectrochim. Acta Part A Mol. Biomol. Spectrosc.* **2013**, *104*, 377–382. [[CrossRef](#)] [[PubMed](#)]
54. Kanga, J.; Liua, Y.; Xiea, M.X.; Lia, S.; Jianga, M.; Wang, Y.D. Interactions of human serum albumin with chlorogenic acid and ferulic acid. *Biochim. Biophys. Acta* **2004**, *1674*, 205–214. [[CrossRef](#)] [[PubMed](#)]
55. Azegami, S.; Tsuboi, A.; Izumi, T.; Hirata, M.; Dubin, P.L.; Wang, B.; Kokufuta, E. Formation of an intrapolymer complex from human serum albumin and poly(ethylene glycol). *Langmuir* **1999**, *15*, 940–947. [[CrossRef](#)]
56. Zhao, L.Z.; Liu, R.T.; Zhao, X.C.; Yang, B.J.; Gao, C.Z.; Hao, X.P.; Wu, Y.Z. New strategy for the evaluation of CdTe quantum dot toxicity targeted to bovine serum albumin. *Sci. Total Environ.* **2009**, *407*, 5019–5023. [[CrossRef](#)] [[PubMed](#)]
57. Wu, D.; Xu, G.; Sun, Y.; Zhang, H.; Mao, H.; Feng, Y. Interaction between proteins and cationic gemini surfactant. *Biomacromolecules* **2007**, *8*, 708–712. [[CrossRef](#)] [[PubMed](#)]
58. Woody, R.W.; Tinoco, I. Optical rotation of oriented helices. III. Calculation of the rotatory dispersion and circular dichroism of the Alpha- and 310-Helix. *J. Chem. Phys.* **1967**, *46*, 4927–4945. [[CrossRef](#)]
59. Taha, M.; Quental, M.V.; Correia, I.; Freire, M.G.; Coutinho, J.A.P. Extraction and stability of bovine serum albumin (BSA) using cholinium-based Good's buffers ionic liquids. *Process Biochem.* **2015**, *50*, 1158–1166. [[CrossRef](#)]
60. Zhang, H.M.; Lou, K.; Cao, J.; Wang, Y.Q. Interaction of a hydrophobic-functionalized PAMAM dendrimer with bovine serum albumin: Thermodynamic and structural changes. *Langmuir* **2014**, *30*, 5536–5544. [[CrossRef](#)] [[PubMed](#)]
61. Flora, K.; Brennan, J.D.; Baker, G.A.; Doody, M.A.; Bright, F.V. Unfolding of acrylodan-labeled human serum albumin probed by steady-state and time-resolved fluorescence methods. *Biophys. J.* **1998**, *75*, 1084–1096. [[CrossRef](#)]
62. Pfeil, W.; Privalov, P.L. Thermodynamic investigations of proteins: II. Calorimetric study of lysozyme denaturation by guanidine hydrochloride. *Biophys. Chem.* **1976**, *4*, 33–40. [[CrossRef](#)]
63. Cai, W.S.; Gan, L.H.; Tam, K.C. Phase transition of aqueous solutions of poly(*N,N*-diethylacrylamide-*co*-acrylic acid) by differential scanning calorimetric and spectrophotometric methods. *Colloid Polym. Sci.* **2001**, *279*, 793–799. [[CrossRef](#)]

64. Keerl, M.; Richtering, W. Synergistic depression of volume phase transition temperature in copolymer microgels. *Colloid Polym. Sci.* **2007**, *285*, 471–474. [[CrossRef](#)]
65. Li, B.; Turuvekere, S.; Agrawal, M.; La, D.; Ramani, K.; Kihara, D. Characterization of local geometry of protein surfaces with the visibility criterion. *Proteins* **2008**, *71*, 670–683. [[CrossRef](#)] [[PubMed](#)]



© 2016 by the authors; licensee MDPI, Basel, Switzerland. This article is an open access article distributed under the terms and conditions of the Creative Commons Attribution (CC-BY) license (<http://creativecommons.org/licenses/by/4.0/>).